Modern Pathology (2015) 28, 575–586

BCOR–CCNB3 fusions are frequent in undifferentiated sarcomas of male children

Tricia L Peters[1,2,9], Vijetha Kumar[1,2,9], Sumanth Polikepahad[1,2], Frank Y Lin[3,4], Stephen F Sarabia[1,2], Yu Liang[5], Wei-Lien Wang[5], Alexander J Lazar[5,6], HarshaVardhan Doddapaneni[7], Hsu Chao[7], Donna M Muzny[7], David A Wheeler[4,7,8], M Fatih Okcu[3], Sharon E Plon[3,4,7,8], M John Hicks[1,2,3,4], Dolores López-Terrada[1,2,3,4], D Williams Parsons[3,4,7,8] and Angshumoy Roy[1,2,3,4]

[1]Department of Pathology, Texas Children's Hospital, Houston, TX, USA; [2]Department of Pathology & Immunology, Baylor College of Medicine, Houston, TX, USA; [3]Department of Pediatrics, Baylor College of Medicine, Houston, TX, USA; [4]Dan L. Duncan Cancer Center, Baylor College of Medicine, Houston, TX, USA; [5]Department of Pathology, University of Texas MD Anderson Cancer Center, Houston, TX, USA; [6]Sarcoma Research Center, University of Texas MD Anderson Cancer Center, Houston, TX, USA; [7]Human Genome Sequencing Center, Baylor College of Medicine, Houston, TX, USA and [8]Department of Molecular and Human Genetics, Baylor College of Medicine, Houston, TX, USA

The *BCOR–CCNB3* fusion gene, resulting from a chromosome X paracentric inversion, was recently described in translocation-negative 'Ewing-like' sarcomas arising in bone and soft tissue. Genetic subclassification of undifferentiated unclassified sarcomas may potentially offer markers for reproducible diagnosis and substrates for therapy. Using whole transcriptome paired-end RNA sequencing (RNA-seq) we unexpectedly identified *BCOR–CCNB3* fusion transcripts in an undifferentiated spindle-cell sarcoma. RNA-seq results were confirmed through direct RT-PCR of tumor RNA and cloning of the genomic breakpoints from tumor DNA. Five additional undifferentiated sarcomas with *BCOR–CCNB3* fusions were identified in a series of 42 pediatric and adult unclassified sarcomas. Genomic breakpoint analysis demonstrated unique breakpoint locations in each case at the DNA level even though the resulting fusion mRNA was identical in all cases. All patients with *BCOR–CCNB3* sarcoma were males diagnosed in mid childhood (7–13 years of age). Tumors were equally distributed between axial and extra-axial locations. Five of the six tumors were soft-tissue lesions with either predominant spindle-cell morphology or spindle-cell areas interspersed with ovoid to round cells. CCNB3 immunohistochemistry showed strong nuclear positivity in five tumors before oncologic therapy, but was patchy to negative in post-treatment tumor samples. An RT-PCR assay developed to detect the fusion transcript in archival formalin-fixed tissue was positive in all six cases, with high sensitivity and specificity in both pre- and post-treated samples. This study adds to recent reports on the clinicopathologic spectrum of *BCOR–CCNB3* fusion-positive sarcomas, a newly emerging entity within the undifferentiated unclassified sarcoma category and describes a simple RT-PCR assay that in conjunction with CCNB3 immunohistochemistry can be useful in diagnosing these tumors.
Modern Pathology (2015) **28,** 575–586; doi:10.1038/modpathol.2014.139; published online 31 October 2014

Undifferentiated unclassified sarcomas constitute a group of rare mesenchymal tumors lacking any evident line of differentiation by standard histopathological, immunophenotypic, ultrastructural, or molecular genetic examination.[1–3] Histologically, undifferentiated/unclassified soft-tissue sarcomas are further subclassified into spindle cell, round cell, epithelioid, and pleomorphic subsets under current World Health Organization guidelines, but individual morphologic patterns often coexist.[1,2,4] This histologic heterogeneity, combined with the absence of a reproducible immunophenotype or specific molecular markers,[1] frequently poses considerable challenges in diagnosis and in predicting clinical behavior.[1–3,5,6] Unclassified sarcomas may also rarely arise in bone as a high-grade pleomorphic sarcoma; however, since the discovery of the *EWSR1*

Correspondence: Dr A Roy, MD, PhD, Department of Pathology & Immunology and Department of Pediatrics, Baylor College of Medicine, Texas Children's Hospital, 1102 Bates Avenue, FC.830, Houston, TX 77030, USA.
E-mail: aroy@bcm.edu
[9]These authors contributed equally to this work.
Received 16 July 2014; revised 9 August 2014; accepted 10 August 2014; published online 31 October 2014

(EWS RNA-binding protein 1)-*ETS* (E26) family gene fusions in Ewing sarcoma, unclassified sarcoma of bone is an infrequent diagnosis.

Unlike other sarcoma subtypes, the taxonomy and diagnosis of which have been refined by the increasing recognition of recurrent molecular genetic aberrations,[1,2,4] the molecular and genetic drivers of undifferentiated unclassified sarcomas remain largely unknown. One such recurrent cytogenetic alteration seen in a subset of 'Ewing sarcoma-like' round-cell undifferentiated sarcomas lacking the pathognomonic *EWSR1-ETS* fusions is the t(4;19)(q35;q13) or t(10;19)(q26.3;q13) translocations, both leading to fusion of *CIC* (capicua homolog) with the *DUX4* (double homeobox 4) gene.[7–13] Round-cell sarcomas with the *CIC–DUX4* fusion may represent a clinically aggressive subset of undifferentiated sarcomas,[8,13,14] and although these tumors share transcriptional subprograms with Ewing sarcoma,[9] distinct immunophenotypic features[15] suggest a discrete pathological entity. Less commonly, the *EWSR1* gene is fused to non-ETS fusion partners (*NFATC2, PATZ1, SP3,* and *SMARCA5*)[16–19] in Ewing-like round-cell undifferentiated sarcomas. However, owing to the rarity of these diagnoses, it remains unclear if these tumors are simply variants of Ewing sarcoma or merit a separate subgrouping.[1,14]

More recently, a novel recurrent paracentric inversion on chromosome X resulting in a *BCOR–CCNB3* fusion gene was identified in ~4% (24/594) of undifferentiated 'Ewing-like' small round-cell sarcomas lacking *EWSR1* gene rearrangements.[20] By gene expression profiling, *BCOR–CCNB3* sarcomas appear distinct from Ewing sarcoma. Moreover, expression of the BCOR–CCNB3 fusion protein appears to drive cell proliferation *in vitro*.[20] Recently, a second series of 10 patients with *BCOR–CCNB3* sarcomas was also reported.[21] Tumors harboring the *BCOR–CCNB3* fusion appear to share some clinical and morphological overlap with the Ewing family of tumors, including the frequent occurrence in long bones of adolescents and young adults, but also appear to have differences, including a strong male predilection and a potentially less aggressive clinical course.[20,21] The identification of a recurrent driver mutation (*BCOR–CCNB3*) and a unique transcriptional profile and immunophenotype[20] in these tumors suggests the emergence of a distinct genetic subgroup of sarcomas that requires further molecular and clinical characterization.

We investigated the prevalence of the *BCOR–CCNB3* fusion in pediatric and adult undifferentiated unclassified sarcomas using a combination of whole transcriptome paired-end next-generation sequencing (whole transcriptome paired-end RNA sequencing (RNA-seq)) and directed RT-PCR, and report on the clinical and histopathological characteristics of six patients with sarcomas harboring this fusion gene. We also report on the development of a targeted RT-PCR assay to detect the *BCOR–CCNB3* fusion in clinical formalin-fixed paraffin-embedded tumor specimens.

Materials and methods

Case Selection

With Institutional Review Board (IRB) approval from Baylor College of Medicine, the Department of Pathology database and consult files at Texas Children's Hospital were searched between 2000–2013 for bone and soft-tissue sarcomas with a final diagnosis containing one of the following search terms: undifferentiated sarcoma; small round blue cell tumor; peripheral primitive neuroectodermal tumor and/or Ewing sarcoma-like tumor; spindle-cell tumor; and sarcoma, not otherwise specified. Tumors that lacked characteristic sarcoma-associated chromosomal translocations or fusion genes by cytogenetics, fluorescence *in situ* hybridization (FISH) and/or RT-PCR (translocation-negative cases) were selected for inclusion in this study. Cases diagnosed as Ewing sarcoma or peripheral primitive neuroectodermal tumor but lacking a pathognomonic *EWSR1* rearrangement were also included. In cases positive for the *BCOR–CCNB3* transcript in post-treated samples, a second search was performed on the entire database to retrieve the pre-treatment diagnostic biopsy, if available. Clinical information (including age, sex, tumor site, treatment, and outcome) and laboratory data were obtained if available from the medical record. A total of 42 cases (23 males and 19 females) were identified for the study, consisting of 31 children (<18 years of age) and 11 adults (range 21–77 years). All adult cases in our consult files were originally diagnosed at the M. D. Anderson Cancer Center. Seven negative controls were also analyzed including six tumors with characteristic molecular genetic aberrations that would not be expected to harbor a *BCOR–CCNB3* fusion: three cases of Ewing sarcoma with pathognomonic *EWSR1* rearrangements, one sarcoma with *CIC* gene rearrangement, an alveolar soft part sarcoma with *ASPSCR1-TFE3* fusion, a mucoepidermoid carcinoma with *MECT1–MAML2* fusion, and a normal tonsil. Clinical features of all 42 cases are described in Supplementary Table S1. In three cases (T149, T150, and T236), biopsies of local recurrences and/or distant metastasis were available and included for evaluation.

RNA-seq

Concurrently with the above study, patients at the Texas Children's Cancer Center are being enrolled in a second IRB-approved protocol for prospective clinical whole-exome sequencing. A substudy of this protocol includes permission to perform other

genomic and RNA analyses for gene discovery. Whole-transcriptome RNA sequencing (RNA-seq) was performed using high-quality total RNA (RIN > 7) extracted from fresh-frozen tissue to prepare strand-specific, poly-A + RNA-seq libraries for sequencing on the Illumina platform (Illumina , San Diego, CA, USA). Briefly, poly-A + mRNA was extracted from 1 μg total RNA, followed by fragmentation and first strand cDNA synthesis. The resultant cDNA was end-repaired, A-tailed, and ligated with Illumina PE adapters. The libraries were sequenced in paired-end mode (2×100-bp reads) on an Illumina HiSeq 2000 platform following amplification on the cBot cluster generation system (Illumina). On an average, over 84 million paired-end reads were generated per sample.

Bioinformatics Analysis

Detection of fusion genes was performed using two independent programs with different algorithms: TopHat-Fusion[22] and deFuse.[23] when using TopHat-Fusion, the FASTQ files were aligned to the reference human genome (hg19) by TopHat (ver. 2.0.10) with fusion-search option on. TopHat-Fusion employs a special-purpose algorithm for filtering spurious candidate fusions including removing multimapped (> 2) reads and pseudogenes, requiring split reads to contain 13-bp of sequence flanking both sides of the fusion junction, filtering intrachromosomal same-strand fusion partners within 100 kb, and retaining candidates supported by evenly distributed reads around junctions that achieve highest scores in a scoring scheme that prefers uniform depth and no gaps or small gaps.[22] Post filtration, candidates were annotated using RefGene and ensGene reference. For deFuse (ver. 0.6.1) analyses, high-quality FASTQ files were subjected to analysis with default options that yielded 969 fusion candidates. Filters to reduce spurious candidates were applied as reported previously.[23] Nominated candidates were further ranked based on location of fusion breakpoints with coding-sequence junctions given highest rank.

RT-PCR and Sanger Sequencing

RNA was extracted from either formalin-fixed, paraffin-embedded tissue using the Ambion RecoverAll Total Nucleic Acid Isolation Kit (Life Technologies, Carlsbad, CA, USA) or fresh-frozen tissue using the mirVana miRNA Isolation Kit (Life Technologies) following the manufacturer's instructions for total RNA isolation. Reverse transcription was performed on 500 ng of total RNA using Superscript III First Strand Synthesis System (Life Technologies) and PCR was performed with HotStarTaq DNA polymerase (Qiagen, Valencia, CA, USA) using primers (*BCOR* exon 15:5′-AGGAGC TGTTAGATCTGGTGGA-3′ and *CCNB3* exon 5:5′-GT GGTTTCTCCATAATGTTTGGT-3′) predicted to generate a 171-bp product. Direct Sanger sequencing was performed using BigDye Terminator v3.1 chemistry (Life Technologies) on positive cases.

Long-Range PCR and Genomic Breakpoint Mapping

Genomic DNA was extracted from fresh-frozen tumor tissue using the QIAamp DNA kit (Qiagen) following the manufacturer's instructions. For amplification of fragments spanning the genomic breakpoints, long-range PCR was performed with primers as published previously[20] using the TaKaRa LA PCR Kit, v2.1 (Clontech Laboratories, Mountain View, CA, USA) and standard conditions. Using the amplified genomic fragment as template, hemi-nested PCR was performed using the *BCOR* exon 15 forward primer and a series of 10 *CCNB3* intron 4 reverse primers successively tiled at ~1 kb intervals along the entire intron. The smallest hemi-nested product generated was then cloned and/or sequenced, followed by a BLAST analysis to identify the genomic coordinates of the breakpoints. The breakpoint junction sequences in *BCOR* and *CCNB3* were identified using long-range PCR and Sanger sequencing. Sequences of breakpoint mapping primers used in long-range PCR are listed in Supplementary Table S2.

FISH

Bacterial artificial clones (BAC) flanking the *BCOR* (RP11-91I16 and RP11-665O2) and *CCNB3* genes (RP11-58H17 and RP11-576P23) on the X chromosome were obtained from the BACPAC Resources Center (bacpac.chori.org) and labeled with Spectrum Green-dUTP and Spectrum Red-dUTP, respectively. Representative sections of formalin-fixed paraffin-embedded tissue were deparaffinized, pretreated at 80 °C for 10 min, subjected to protease digestion for 3–7 min at 37 °C, dehydrated, air-dried, and hybridized overnight at 37 °C to labeled probes followed by washes at 73 °C. Slides were evaluated for the appearance of a bicolor doublet or a fused signal using a fusion probe approach.

Histology Review and Immunohistochemistry

All cases were reviewed for histomorphologic features, including architectural pattern, presence of necrosis, nuclear features, and mitoses. Cases positive for the *BCOR–CCNB3* fusion underwent independent review by three independent soft-tissue pathologists (WLW, AJL, and MJH). Representative 4-μm thick sections of the diagnostic biopsy and recurrent specimens of the positive cases were stained with a rabbit polyclonal antibody to CCNB3 (clone HPA000496; Sigma-Aldrich, St Louis, MO, USA) at a 1:200 dilution.

Results

Identification of a *BCOR–CCNB3* Fusion Transcript by RNA-seq

To identify novel fusion genes in undifferentiated unclassified sarcomas, we performed RNA-seq. In an undifferentiated spindle-cell sarcoma, not otherwise specified, arising in an 11-year-old male (case T107), RNA-seq analysis generated 82.8 million paired-end purity-filtered reads of which 1002 split reads were found to span the junction between *BCOR* exon 15 and *CCNB3* exon 5, producing an in-frame chimeric transcript. In addition, 304 high-quality spanning mate–pairs were identified with one-read mapping to *BCOR* exon 15 and the mate-pair mapping to *CCNB3* exon 5 (Figure 1). All fusion-supporting RNA-seq reads contained an identical fusion junction.

We confirmed the RNA-seq result for the *BCOR–CCNB3* fusion using specific primers for *BCOR* exon 15 and *CCNB3* exon 5 in RT-PCR experiments to amplify a 171-bp product that on sequencing revealed an in-frame fusion of the second base in the last codon of *BCOR* (hg19; chrX:39 911 366) and the first base of *CCNB3* exon 5 (chrX:50 051 505) (Figure 1). As reported previously,[20] the fusion sequence is compatible with an aberrant splicing event due to activation of a cryptic 'GT' splice donor site encompassing the last codon and the termination codon of *BCOR* (Figure 1). The fusion was not detected by RT-PCR analysis of a patient-matched lymphoblastoid cell line, indicating that it was a somatic (tumor-specific) event. To confirm this observation, we analyzed the genomic breakpoints between *BCOR* and *CCNB3* using long-range PCR experiments (Figure 2). Using previously published

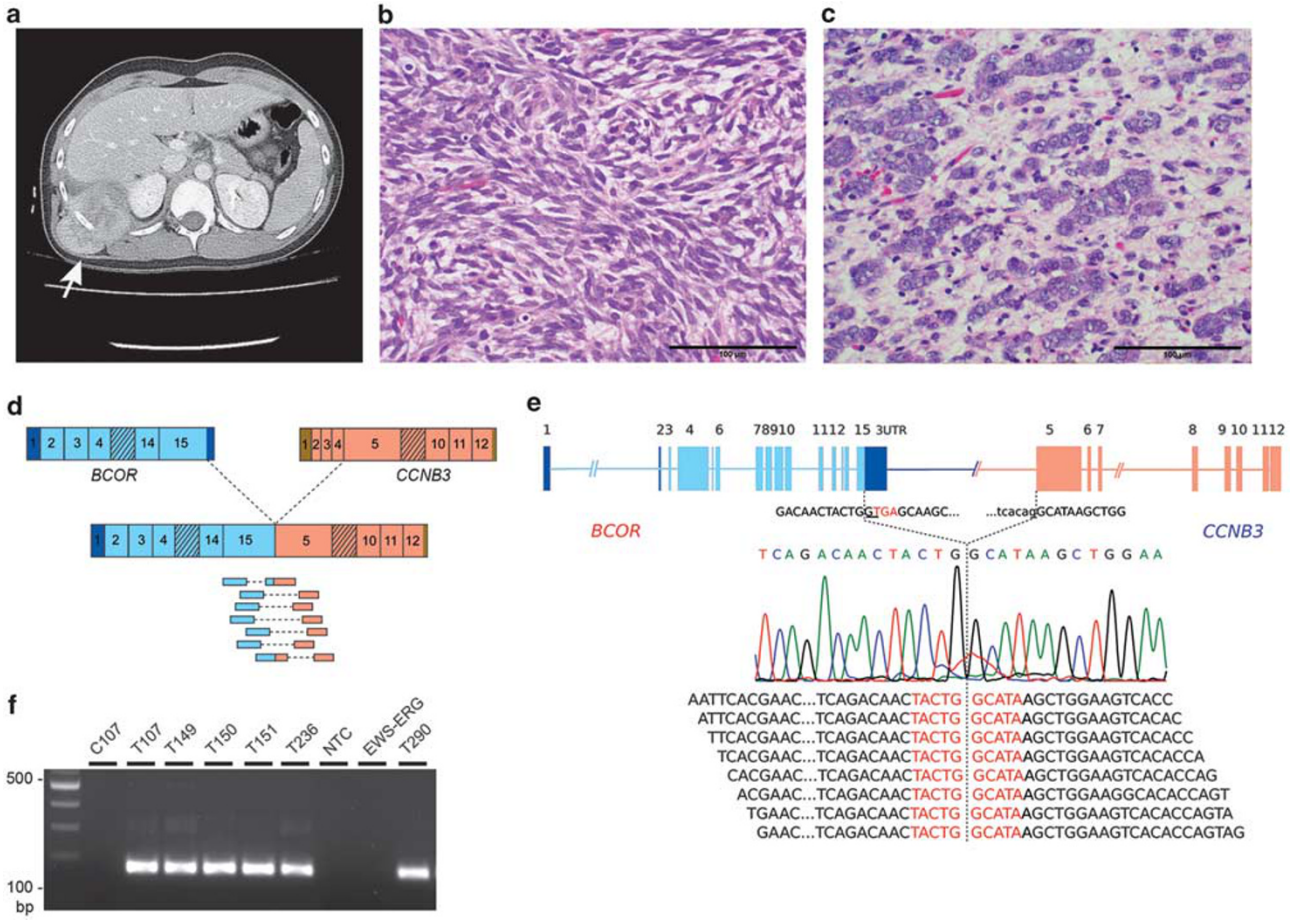

Figure 1 Identification of the *BCOR–CCNB3* fusion in sarcomas. (**a**) Axial CT in a 7-year-old male shows a right-sided soft tissue mass (T107) abutting the ninth rib (white arrow). (**b**) Diagnostic pretreatment biopsy demonstrating the index case (T107) to be an unclassified spindle-cell sarcoma (H&E stain). (**c**) The post-chemotherapy specimen shows more frequent rounded cells forming nests in a background of edematous to myxoid stroma. (**d**) Schematic depicting the distribution of paired-end split and spanning RNA-seq reads joining *BCOR* exon 15 with *CCNB3* exon 5. (**e**) Direct sequencing confirms the RNA-seq reads; the *BCOR–CCNB3* fusion transcript is a result of a cryptic 'GT' (underlined) splice donor site activation in BCOR exon 15 leading to skipping of the termination 'TGA'. (**f**) RT-PCR with fusion-specific primers shows expression of a 171-bp band only in the tumor (T107) but not in a lymphoblastoid cell line from matched peripheral blood (C107). Additional cases of undifferentiated unclassified sarcoma expressing the *BCOR–CCNB3* fusion (T149, T150, T151, T236, T290), which is not expressed in an Ewing sarcoma with *EWSR1-ERG* translocation (EWS-ERG). NTC, no template control.

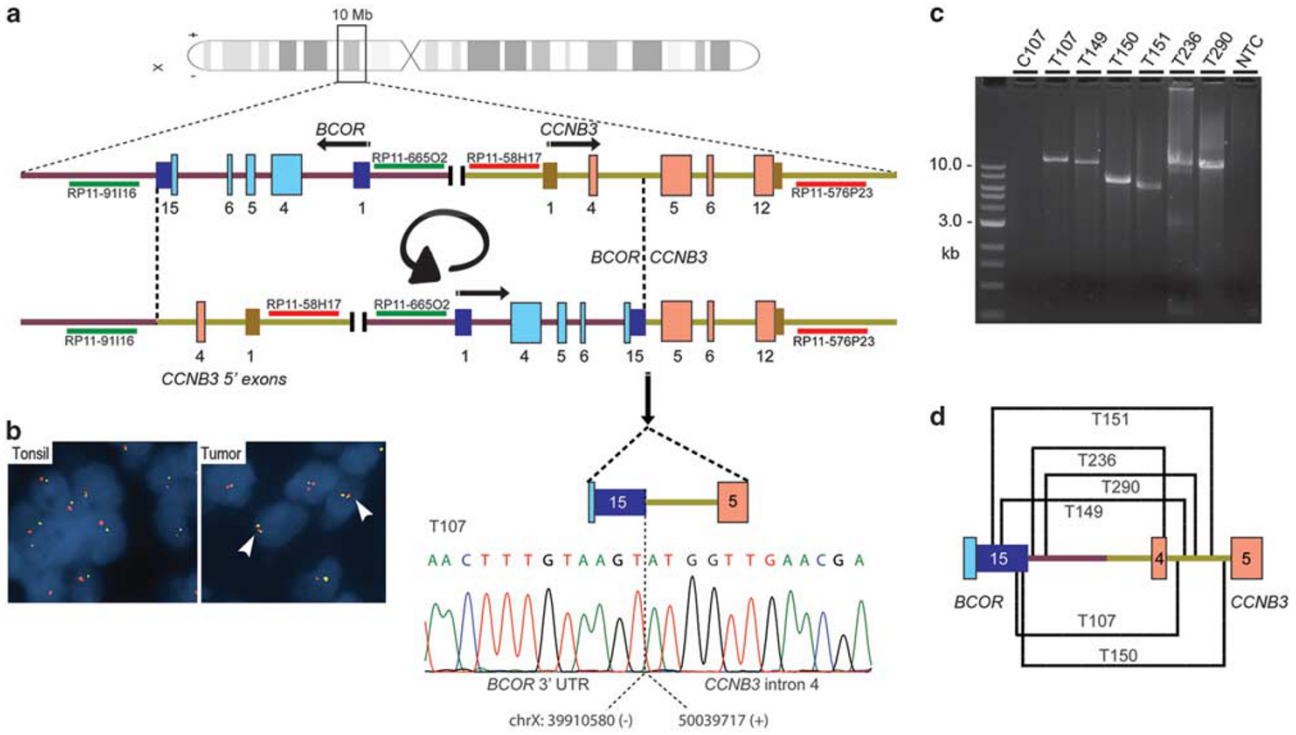

Figure 2 Genomic rearrangement in *BCOR–CCNB3* sarcomas. (**a**) Schematic depicting the paracentric inversion on chromosome X. *BCOR* and *CCNB3* are transcribed in opposite directions. The locations of the BACs used for FISH analysis are shown. Dashed lines indicate the genomic breakpoints for the inversions at the *BCOR* 3′UTR or downstream region and in intron 4 of *CCNB3*. The electropherogram depicts the sequence context of the genomic breakpoint in T107. (**b**) Interphase FISH using probes labeled in Spectrum-Green and Spectrum-Red show two unicolor signals in normal tonsil cells, whereas in *BCOR–CCNB3* sarcoma cells, bicolor doublets (white arrowheads) are seen. (**c**) Long-range PCR amplification using primers in *BCOR* and *CCNB3* or hemi-nested PCR using *CCNB3* intron 4 primers show specific amplification of genomic DNA fragments of different sizes from all 6 tumors with *BCOR–CCNB3* fusion transcripts, but not from matched lymphoblastoid cell line DNA (C107) for the index case (T107). (**d**) Schematic depicting the genomic breakpoint locations for the rearrangements in each case.

primers,[20] long-range PCR amplified a specific product (>12 kb) only from the tumor DNA but not from the patient-matched lymphoblastoid cell line, confirming the somatic nature of the genomic rearrangement. Primer walking using a series of reverse primers tiled on *CCNB3* intron 4 was performed to map the genomic breakpoint on chromosome X at the *BCOR* 3′UTR (chrX:39 910 580) and *CCNB3* intron 4 (chrX:50 039 717) (Figure 2).

Prevalence of *BCOR–CCNB3* in Undifferentiated Unclassified Sarcomas in Children and Adults

Using the RT-PCR assay described above, we assessed the prevalence of the *BCOR–CCNB3* transcript in archived pediatric and adult cases of undifferentiated unclassified sarcomas. In 41 additional sarcoma cases that met the inclusion criteria (see Methods and Supplementary Table S1), RT-PCR on either frozen or formalin-fixed paraffin-embedded specimens (depending on availability) followed by direct sequencing identified an additional five cases that were positive for the *BCOR–CCNB3* fusion (Table 1; Figures 1 and 2). As in case T107 described above, the chimeric transcript joined the last codon of *BCOR* to exon 5 of *CCNB3* in all cases. Notably, the fusion transcript was also identified in all available subsequent tissue specimens from these patients including local recurrences and distant metastases. RT-PCR for *BCOR–CCNB3* was appropriately negative in seven specimens included as negative controls (see Methods). As described above, long-range PCR was used to characterize the X chromosome breakpoints of the inversions, resulting in amplified genomic fragments of varying sizes and mapping of the breakpoints to unique locations within the *BCOR* 3′ UTR, the *BCOR-MID1IP1* intergenic region, *CCNB3* exon 4 and *CCNB3* intron 4 (Supplementary Table S3; Figure 2d and Supplementary Figure 1). In addition, FISH performed on two *BCOR–CCNB3*-positive cases with dual-color probes on chromosome X[20] detected a bicolor doublet in both cases (Figure 2). In total, *BCOR–CCNB3* fusion transcripts were identified in 6 of 42 undifferentiated unclassified sarcomas (14.3%) examined by RNA-seq and RT-PCR.

Histopathology of *BCOR–CCNB3* Fusion-Positive Sarcomas

A review of the pretreatment diagnostic biopsy specimens from the six *BCOR–CCNB3*-positive cases showed tumors of variable cellularity (Figure 3). The

Table 1 Morphological, immunophenotypic and molecular features of *BCOR–CCNB3* fusionpositive sarcomas

Patient	*Tumor site*	*Histopathology*	*Mitoses/ 10 hpf*	*Necrosis*	*Immunophenotype*	*Karyotype*	*FISH*	*PCR*	*Diagnosis*	*CCNB3 IHC*
T107	Soft tissue, chest wall	Spindle cells in a storiform pattern with dispersed chromatin and inconspicuous nucleoli	13	Yes	CD117$^+$, fascin$^+$	46, XY	FOXO1$^-$, SYT$^-$, EWSR1$^-$	Neg: COL1A1-PDGFB	Spindle-cell sarcoma, NOS	POS
T149	Calcaneus	Ovoid cells with finely dispersed chromatin and inconspicuous nucleoli	40	No	CD99$^+$ (w)	46, XY, t(5;9)(q22;q32)	ND	ND	PNET	NEG
T150	Soft tissue, ankle	Small round and spindle cells	16	No	bcl-2$^+$, vim$^+$, CD99$^+$ (w)	46, XY	EWSR1$^-$	Neg: EWSR1-FLI1/ ERG; SYT-SSX	Sarcoma, NOS	POS
T151	Soft tissue, paraspinal	Atypical cells inconspicuous nucleoli	5	No	vim$^+$, CD56$^+$; CD99$^-$	46, XY, inv (9)(p11q12)	ND	ND	Sarcoma, NOS	POS
T236	Pelvis	Ovoid to spindle cells with fine chromatin and inconspicuous nucleoli	30	Yes	CD99$^+$ (w), vim$^+$	46, XY	ND	Neg: EWSR1-FLI1/ ERG; PAX3/7-FOXO1	Undifferentiated sarcoma	POS
T290	Soft tissue	Spindle cells with eosinophilic cytoplasm in a myxoid matrix	1	Yes	CD99$^+$ (w), vim$^+$	46, XY	FOXO1$^-$, SYT$^-$, EWSR1$^-$	Neg: FUS-CREB3L1/ L2	Spindle-cell neoplasm	POS

Abbreviations: FISH, fluorescence *in situ* hybridization; IHC, immunohistochemistry; Neg, negative; NOS, not otherwise specified; PNET, peripheral primitive neuroectodermal tumor; vim, vimentin.

tumors were comprised of areas with high cellularity alternating with less cellular areas in which discohesive neoplastic cells were embedded, often in an edematous and myxoid stroma containing occasionally angulated thin-walled vessels. The original diagnosis for two tumors was spindle-cell sarcoma and spindle-cell neoplasm (T107 and T290, respectively); both tumors contained areas with a prominent spindle-cell pattern and in the case of T107, were arranged in a vague fascicular architecture. The other *BCOR–CCNB3*-positive tumors were composed of tumor cells with variable nuclear features and included spindled, angulated, and ovoid cells overlapping with areas of round-cell morphology (Figure 3). Tumor cells had scant to moderate amounts of eosinophilic cytoplasm, and irregular nuclear contours. Nuclei were vesicular with finely dispersed chromatin and occasional indistinct to small nucleoli (as in case T290). None of the tumors showed bizarre nuclear pleomorphism that would be more compatible with a diagnosis of undifferentiated pleomorphic sarcoma. Areas of necrosis were seen in three tumors, ranging from focal to 50% of the tumor area. Mitotic activity, except for T290, was often brisk in the pretreatment tumors (Table 1), with a median of 30 mitoses per 10 high-power fields (range 1–40).

In two cases (T150 and T290), additional pretreatment resection specimens were available following the diagnostic biopsy, highlighting the variable cellular morphology of these tumors. T150 was originally diagnosed as sarcoma, not otherwise specified on biopsy, but the resection specimen consisted of predominantly ovoid to stellate to epithelioid cells in a myxoid and occasionally collagenous stroma and the tumor was reclassified as consistent with epithelioid fibrosarcoma. T290 was embolized before resection, which may have affected the histopathologic features; nevertheless the resection had areas with higher cellularity and mitotic activity (16 per 10 high-power fields) compared with the preceding diagnostic biopsy.

Post-treatment samples were available for evaluation in four cases, including three relapsed tumor specimens (T149, T150, and T236). In each of the relapsed cases, tumor cell morphology was similar to the corresponding pretreatment samples (Figure 3). Interestingly, in T107, the resection specimen immediately following treatment showed similar spindle-cell morphology as in the diagnostic biopsy, but also showed areas with tumor cells with distinctly larger rounded nuclei (Figure 1c).

Immunohistochemistry performed as part of the diagnostic work-up showed no specific reproducible immunophenotype. CD99 staining was weak to negative in all tumors. Staining for CCNB3, however, showed strong and diffuse nuclear positivity along with patchy cytoplasmic staining in five tumors (Figure 4). In one tumor diagnosed in 1993 (T149), the pretreatment biopsy specimen stained only patchily with the CCNB3 antibody, and the

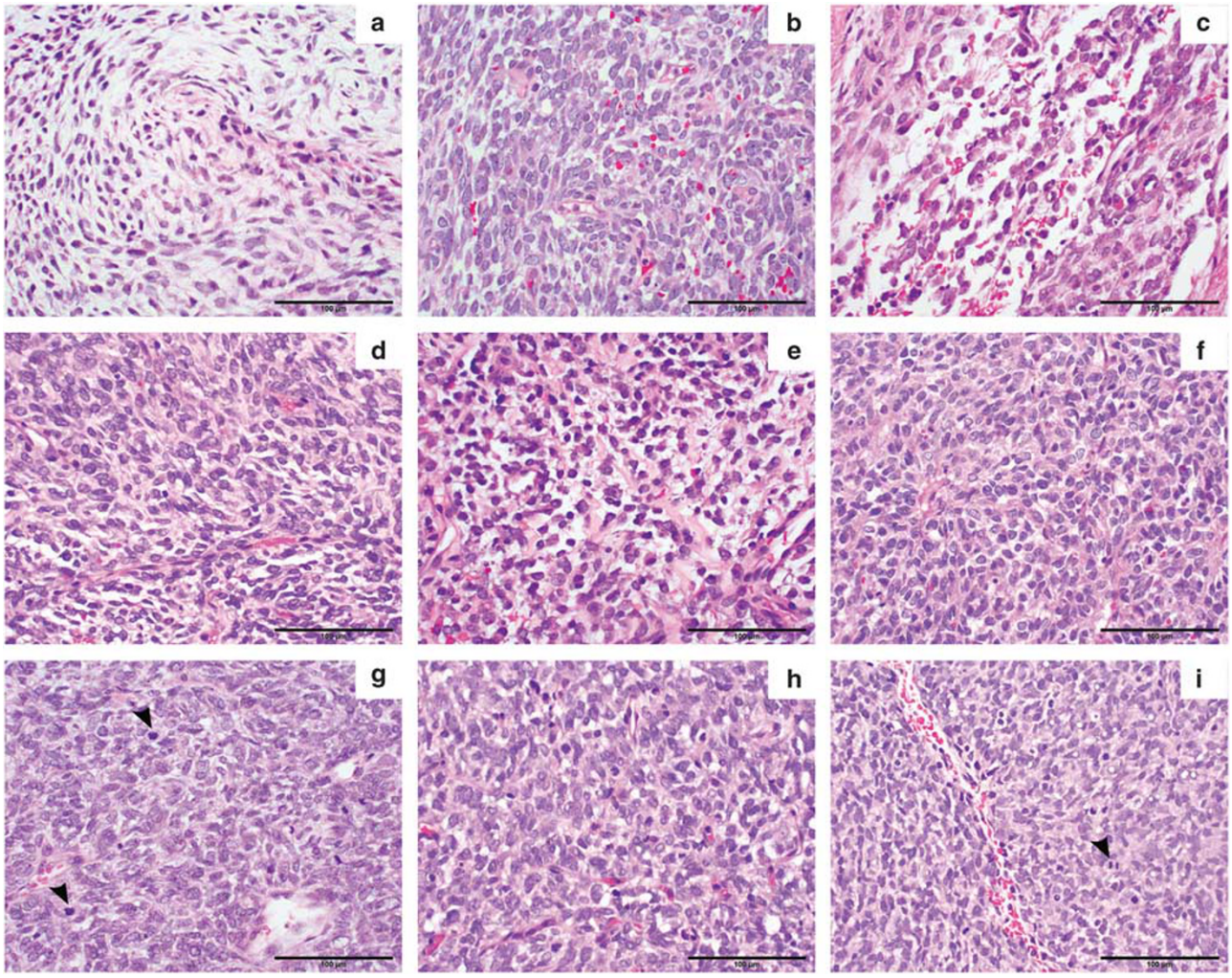

Figure 3 Histological features of *BCOR–CCNB3*-positive sarcomas. (**a**, **b**) Spindle-cell neoplasm (T290) in a myxoid to edematous matrix with more ovoid cells in (**b**). (**c**) Undifferentiated sarcoma (T151) with angulated and ovoid cells. (**d–f**) Pretreatment (**d**, **e**) and the post-treatment relapsed specimen (**f**) from T150 shows angulated, spindle, and round cells with similar morphology. (**g**, **h**) The pretreatment sample (**g**) for T149 shows similar features compared with the post-treatment relapse (**h**) after 8 years off therapy (arrowheads scattered mitoses). (**i**) T236 with histologic features of undifferentiated sarcoma similar to the other *BCOR–CCNB3* cases. Scale bars, 100 μm.

post-treatment specimen was completely negative. In two other cases (T150 and T236) with strong CCNB3 staining pretreatment, the post-treatment resection specimens were only patchily positive or negative. In three negative controls tested (two Ewing sarcomas and one *CIC*-rearranged sarcoma), CCNB3 staining was either absent (Figure 4h) or patchy cytoplasmic, although nuclear expression could be focally seen in one Ewing sarcoma (Figure 4i).

Clinical Features of *BCOR–CCNB3* Fusion-Positive Sarcomas

A review of the clinical features of the six patients identified with *BCOR–CCNB3* sarcoma revealed that all were male, diagnosed in mid childhood (ages 7–13 years), and presented with nonmetastatic disease (Table 2). Tumors were equally distributed between axial (paraspinal, chest wall, and pelvis) and extra-axial (ankle, calcaneus, and thigh) locations. Five of six cases appeared to be of soft tissue origin without extensive involvement of bone by imaging and gross examination of the resection specimen (when available). Gross total resection was achieved in four of six patients, including all three extra-axial tumors. One patient (T290) with a completely resected tumor transferred care to another institution shortly following surgical resection and details of adjuvant therapy are unavailable. Adjuvant and/or neoadjuvant therapy was administered to four of five patients, including chemotherapy and involved-field radiation therapy in three patients and chemotherapy alone in one patient (Table 2). All three patients with axial tumors received adjuvant chemotherapy and radiation therapy. Adjuvant chemotherapy backbones were diverse, consisting of regimens based on protocols for non-rhabdomyosarcoma soft-tissue sarcoma for two

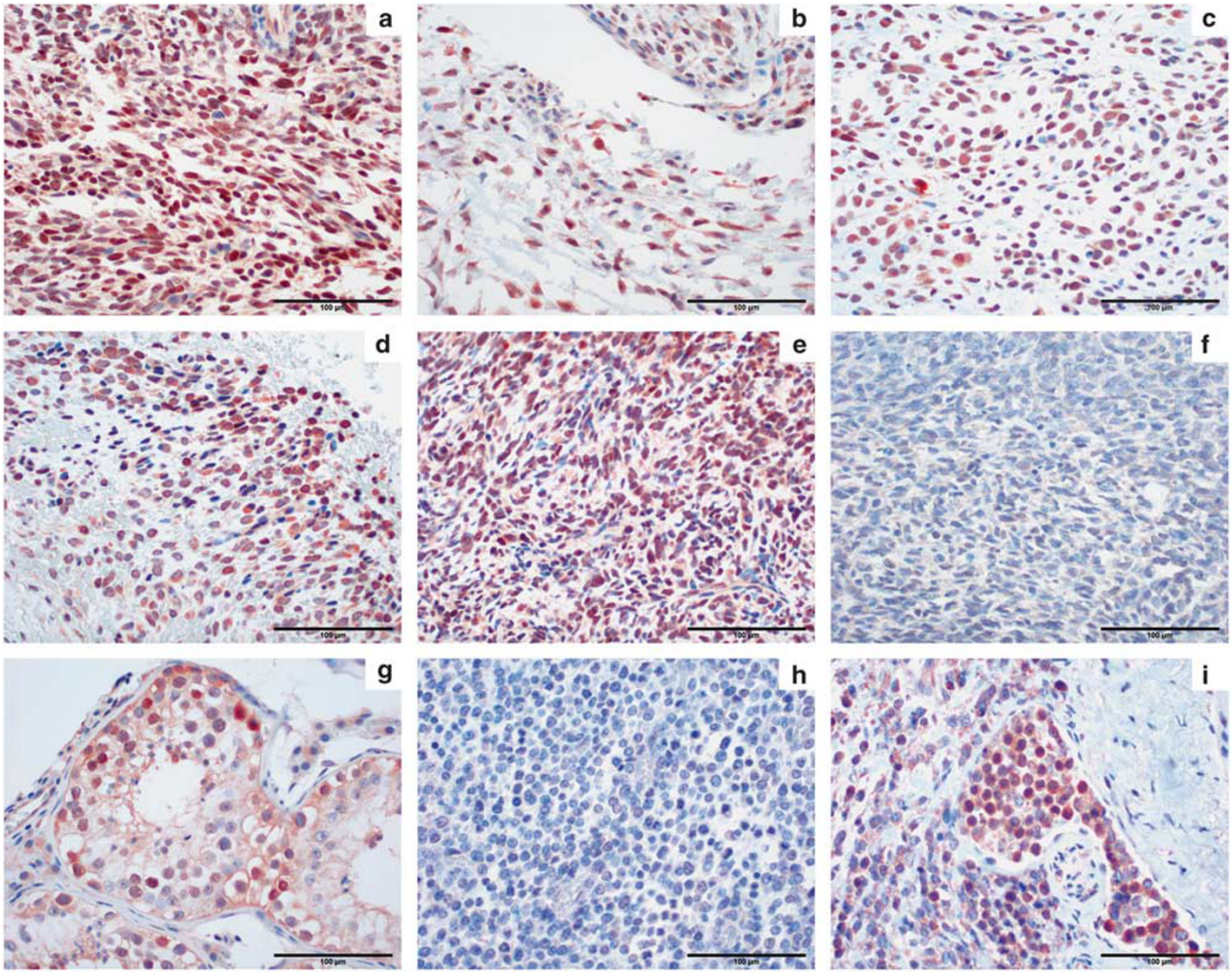

Figure 4 CCNB3 expression in *BCOR–CCNB3*-positive sarcomas. Nuclear CCNB3 immunopositivity is strong and diffuse (**a**, **b**, **c**, and **e**), strong but patchy (**d**) and negative in T149 (**f**). CCNB3 expression in spermatocytes (**g**) serves as a control. A *CIC*-rearranged small round-cell tumor is expectedly negative (**h**); however, strong patchy nuclear expression is seen in a Ewing sarcoma tumor (**i**). Scale bars, 100 μm.

patients (ifosfamide and doxorubicin), Ewing sarcoma for one patient (vincristine, dactinomycin, cyclophosphamide, adriamycin, ifosfamide, and etoposide), and rhabdomyosarcoma for one patient (vincristine, dactinomycin, and cyclophosphamide). At a median follow-up of 63 months (range 3–157 months), three patients developed recurrent disease at 9, 25, and 98 months from diagnosis and two subsequently died of progressive disease (Table 2). Both patients who died from progressive disease had undergone a complete resection of an extra-axial tumor with one having received no neoadjuvant or adjuvant therapy and the other having received adjuvant chemotherapy based on an Ewing protocol.

Discussion

Historically, recurrent chromosomal translocations in sarcomas were discovered through conventional karyotyping and FISH. In recent years, the emergence of next-generation genomic sequencing technologies, and in particular RNA-seq, has led to the discovery of previously unrecognized cryptic intrachromosomal rearrangements (inversions, deletions, and segmental duplications) producing novel oncogenic fusion genes in sarcomas,[24–26] including the recent identification of the *BCOR–CCNB3* gene fusion in 'Ewing-like' sarcomas in 2012.[20] Since this original description by Pierron *et al*,[20] a second series of 10 sarcomas with the *BCOR–CCNB3* fusion in translocation-negative sarcomas has recently been reported.[21] In the present study, we initially used RNA-seq to identify a *BCOR–CCNB3* fusion gene in an unclassified spindle-cell sarcoma. This prompted us to screen for additional cases of the *BCOR–CCNB3* fusion in translocation-negative undifferentiated unclassified sarcomas arising in either bone or soft tissue to further characterize the pathology and clinical course of sarcomas harboring this newly discovered fusion gene.

Table 2 Clinical features of patients with *BCOR–CCNB3* sarcomas

Patient	*Age at diagnosis (years)*	*Gender*	*Bone or soft tissue*	*Site*	*Anatomic location*	*Metastatic at diagnosis*	*Initial resection*	*Maximum resection*	*Adjuvant therapy*	*Chemotherapy backbone*	*Diagnosis to recurrence (months)*	*Diagnosis to last contact (months)*	*Status at last contact*
T107	11	M	ST	Axial	Chest Wall	No	Biopsy	GTR	C,X	NRSTS	NA	11	NED
T149	7	M	Bone	Ext	Calcaneus	No	Biopsy	GTR	C	EWS	98	157	DOD
T150	13	M	ST	Ext	Ankle	No	GTR	GTR	None	N/A	9	34	DOD
T151	10	M	ST	Axial	Paraspinal	No	STR	STR	C,X	NRSTS	NA	94	NED
T236	10	M	ST	Axial	Pelvis	No	Biopsy	Biopsy	C,X	RMS	25	93	NED
T290	7	M	ST	Ext	Thigh	No	GTR	GTR	ND	ND	NA	3	NED

Abbreviations: C, chemotherapy; DOD, dead of disease; EWS, Ewing sarcoma chemotherapy with vincristine, dactinomycin, cyclophosphamide, adriamycin, ifosfamide, etoposide; Ext, extra-axial; GTR, gross total resection; M, male; NA, not applicable; NED, no evidence of disease; ND, not determined; NRSTS, nonrhabdomyosarcoma soft tissue sarcoma chemotherapy with ifosfamide/doxorubicin; RMS, rhabdomyosarcoma chemotherapy with vincristine, dactinomycin, cyclophosphamide; ST, soft tissue; STR, subtotal resection; X, radiation therapy.
Initial resection denotes extent of surgical resection prior to adjuvant therapy.

One of the cases in this series (T149) appeared to arise in the calcaneus on imaging. Biopsy of the large soft-tissue extension was diagnosed as a peripheral primitive neuroectodermal tumor in 1993, before routine availability of ancillary FISH and molecular diagnostic techniques, and is similar to the majority of *BCOR–CCNB3*-positive sarcomas reported by Pierron *et al*[20] and Puls *et al*.[21] This tumor consisted of round to ovoid cells with fine chromatin, but also spindled areas on close examination that would be unusual for conventional Ewing sarcoma/peripheral primitive neuroectodermal tumor and would be more compatible as an atypical variant. However, in contrast to the two published series that reported the majority of cases to be bone tumors, five of the six cases in this series, including the index case (T107), were originally diagnosed as unclassified undifferentiated soft-tissue sarcomas (Table 1). The morphologic features of these five cases varied from predominantly spindle-cell morphology (T107, T290) to cases with ovoid and angulated cells interspersed with areas of spindle-cell morphology, a pattern unusual for either classic Ewing sarcoma or the emerging entity of *CIC–DUX4*-positive sarcomas, both of which are characterized by more uniform small round-cell morphology. In both T107 and T290, several spindle-cell lesions were considered in the differential diagnosis, including synovial sarcoma, dermatofibrosarcoma protuberans, and low-grade fibromyxoid sarcoma; however, these diagnoses were ruled out through molecular testing for the respective fusion transcripts. In fact, independent expert review of T290 led to reclassification of this tumor as an intermediate-grade myofibroblastic sarcoma, and the untreated resection specimen from T150 was diagnosed as an epithelioid fibrosarcoma, further highlighting the frequency of spindle-cell morphology in these tumors. Significantly, in the two previously published series,[20,21] between 25 and 50% of cases were described as having a spindle-cell histology, including 'fusiform' cell sarcoma, malignant peripheral-nerve sheath tumor, synovial sarcoma or simply primitive spindle-cell sarcomas. On the basis of these previous reports as well as our data, it is clear that *BCOR–CCNB3* fusion-positive sarcomas can be characterized by spindle-cell morphology that can be predominant or focal in distribution intermixed with areas with round or ovoid cells. It is therefore of practical relevance to emphasize that these tumors are not merely 'Ewing-like' sarcomas within the small blue round-cell bone tumor category,[1,13,14] but can present as unclassified undifferentiated spindle-cell sarcomas.

Identification of recurrent and specific diagnostic markers is particularly relevant for pathologists attempting to classify undifferentiated sarcomas, a diagnosis of exclusion that is influenced by the availability (or lack thereof) of advanced diagnostic tools, such as electron microscopy and molecular genetic testing.[1,2] Although undifferentiated

sarcomas have long been recognized as a heterogeneous group of tumors, the recent application of molecular genetic techniques is further refining this category into genetic subgroups.[2,4] This has led to a steady decline in the proportion of childhood sarcomas diagnosed as undifferentiated unclassified sarcomas,[3,27] with best estimates being that these tumors comprise approximately 5–10% of childhood sarcomas in the Intergroup Rhabdomyosarcoma Study I and II.[28] With the current study, 6 of 42 undifferentiated unclassified sarcomas proved to be BCOR–CCNB3 fusion-positive sarcomas, representing 14% of all undifferentiated unclassified sarcomas in our cohort. It remains critical to attempt further reproducible subclassification of this heterogeneous group to study the clinicopathologic behavior of the different subsets.[2] Although the specificity and clinical utility of CCNB3 immunohistochemistry as a diagnostic tool needs to be more thoroughly investigated, we confirm in this study previous reports proposing the CCNB3 antibody as a potentially useful adjunct tool in diagnosing this entity,[20,21] with five of six pretreatment cases showing nuclear CCNB3 expression although staining was patchy in post-treatment samples. We cannot exclude the possibility that the absence of CCNB3 immunopositivity in the one pretreatment diagnostic biopsy in our series (T149) was due to the age of the formalin-fixed paraffin-embedded tissue block (21 years). Significantly, however, an RT-PCR assay for detecting the *BCOR–CCNB3* fusion in formalin-fixed paraffin-embedded as well as in frozen tumor tissue was able to reproducibly and robustly detect the fusion transcript in all cases (including the formalin-fixed paraffin-embedded block from T149), including recurrent and metastatic tumor samples, even in those with ambiguous or negative CCNB3 immunostaining. RT-PCR for *BCOR–CCNB3* was appropriately negative in six negative controls, suggesting that molecular testing for this fusion can be a highly sensitive and specific diagnostic tool.

Several clinical features of *BCOR–CCNB3* sarcomas appear somewhat distinctive when compared with entities most likely to be in the differential diagnoses of these lesions, including Ewing sarcoma and *CIC–DUX4*-positive sarcomas. First, as in previous reports,[20,21] *BCOR–CCNB3* fusion-positive sarcomas in this series were seen predominantly in older children. At diagnosis, all six positive cases in our series were in children aged 7–13 years; taken together with the previously reported cases, these tumors appear to predominantly occur in children and adolescents (87% (35/40) in patients between 6 and 18 years of age), an age distribution more similar to that of classical Ewing sarcoma[1] than *CIC–DUX4* sarcomas (median age 24 years).[13,14] Second, all six *BCOR–CCNB3*-positive cases in our series were males, and together with the cases published to date, 78% of cases (31/40) have now been reported in males (M:F ratio of 3.4:1), a far greater male predominance than in Ewing sarcoma (1.4:1)[1] or *CIC*-rearranged tumors ($\sim$1:1).[13] Indeed the prevalence of *BCOR–CCNB3* fusion-positive sarcomas among male children $<$18 years age in our series is 35.3% (6/17), a remarkably high frequency for this genetic subgroup among translocation-negative undifferentiated unclassified sarcomas within this patient demographic. A high predominance of X chromosome inversions arising in the male germline and resulting in hemophilia A has been hypothesized to be related to the inability of the single X chromosome in males to use the homologous X chromosome as a template for recombination-mediated repair during meiosis.[29] It is unclear if a similar mechanism exists for mitotic recombination in somatic cells. Third, *BCOR–CCNB3* sarcomas appear to arise in either bone or soft tissue, similar to Ewing sarcoma/peripheral primitive neuroectodermal tumor but distinct from *CIC–DUX4*-positive sarcomas, which have been exclusively reported in soft tissues.[7,8,13,14]

The clinical outcomes for patients with *BCOR–CCNB3* are currently unclear, given the small number of such patients reported to date and the heterogeneity of treatment regimens administered. Previous reports have described survival as not significantly different than for patients with Ewing sarcoma,[21] which is broadly consistent with the outcomes observed in the current series. Although none of our six *BCOR–CCNB3*-positive patients were observed to have metastatic disease at diagnosis, of the four patients followed for $>$1 year, three have recurred (at 9, 25, and 98 months from diagnosis) and two have died of disease (at 34 and 157 months). Of note, both of the patients who died initially underwent a total resection of an extra-axial tumor. On the other hand, both patients for whom subtotal resections were initially achieved are alive without evidence of disease at 93 and 94 months following diagnosis, including one patient (T236) whose tumor recurred at 25 months. Identification of additional cases is necessary before any definitive assessment can be made regarding the clinical behavior of *BCOR–CCNB3* fusion-positive sarcomas.

The pathogenic role of *BCOR–CCNB3* fusions in sarcomas remains to be determined. Whereas CCNB3 is thought to be a meiotic cyclin restricted to spermatocytes, the *BCOR* gene, originally discovered to encode a nuclear corepressor of BCL6, regulates mesenchymal stem-cell function through epigenetic modification of histone methylation.[30] The expression of the *BCOR–CCNB3* fusion gene in undifferentiated unclassified sarcomas is therefore consistent with the presumed activity of the BCOR promoter in putative mesenchymal progenitor cells. Given that the entire BCOR protein is part of the putative fusion oncoprotein, further studies are needed to investigate the specific role of the different domains in BCOR. Remarkably for a fusion gene partner, BCOR has been identified as both the N-terminal partner (*BCOR-RARA* in acute

promyelocytic leukemia[31]) as well as the C-terminal partner (*ZC3H7B-BCOR* in endometrial stromal sarcoma[32] and ossifying fibromyxoid tumor[33]) in different cancers suggesting alternate mechanisms for oncogenesis in these tumors.

The practical utility of subclassifying undifferentiated/unclassified tumors into genetic subgroups lies in appropriate risk stratification and development of therapeutic approaches targeted towards the specific fusion transcripts and/or downstream signaling pathways regulated by the fusion gene. This report adds to the growing body of evidence that *BCOR–CCNB3* sarcomas are predominantly seen in male children, and suggest that this diagnosis be strongly considered in males diagnosed with translocation-negative undifferentiated unclassified spindle-cell sarcomas and not only tumors with Ewing-like morphology. Routine molecular diagnosis of this entity using RT-PCR either alone or in combination with CCNB3 immunohistochemistry, is the most reproducible diagnostic approach for these tumors and would provide additional cases for future studies to determine risk stratification, outcome, and targeted therapy.

Acknowledgments

We acknowledge Angela Major and E Faith Hollingsworth for technical assistance. The studies were supported by Dan L Duncan Cancer Center Multi-Investigator Pilot Project, NHGRI/NCI 1U01HG006485 and the Cancer Prevention & Research Institute of Texas (CPRIT) RP120685.

Disclosure/conflict of interest

The authors declare no conflict of interest.

References

1 Fletcher CDM, Chibon F, Mertens F. Undifferentiated/unclassified sarcomas, In: Fletcher CDM, Bridge JA, Hogendoorn PCW, Mertens F (eds). WHO classification of tumours of soft tissue and bone, 4th edn. IARC Press: Lyon, France; 2013, pp 235–238.
2 Fletcher CD. Undifferentiated sarcomas: what to do? And does it matter? A surgical pathology perspective. Ultrastruct Pathol 2008;32:31–36.
3 Alaggio R, Bisogno G, Rosato A, *et al.* Undifferentiated sarcoma: does it exist? A clinicopathologic study of 7 pediatric cases and review of literature. Hum Pathol 2009;40:1600–1610.
4 Fletcher CD. The evolving classification of soft tissue tumours—an update based on the new 2013 WHO classification. Histopathology 2014;64:2–11.
5 Pawel BR, Hamoudi AB, Asmar L, *et al.* Undifferentiated sarcomas of children: pathology and clinical behavior–an intergroup rhabdomyosarcoma study. Med Pediatr Oncol 1997;29:170–180.
6 Somers GR, Gupta AA, Doria AS, *et al.* Pediatric undifferentiated sarcoma of the soft tissues: a clinicopathologic study. Pediatr Dev Pathol 2006;9:132–142.
7 Graham C, Chilton-MacNeill S, Zielenska M, *et al.* The CIC-DUX4 fusion transcript is present in a subgroup of pediatric primitive round cell sarcomas. Hum Pathol 2012;43:180–189.
8 Italiano A, Sung YS, Zhang L, *et al.* High prevalence of CIC fusion with double-homeobox (DUX4) transcription factors in EWSR1-negative undifferentiated small blue round cell sarcomas. Genes Chromosomes Cancer 2012;51:207–218.
9 Kawamura-Saito M, Yamazaki Y, Kaneko K, *et al.* Fusion between CIC and DUX4 up-regulates PEA3 family genes in Ewing-like sarcomas with t(4;19)(q35;q13) translocation. Hum Mol Genet 2006;15:2125–2137.
10 Rakheja D, Goldman S, Wilson KS, *et al.* Translocation (4;19)(q35;q13.1)-associated primitive round cell sarcoma: report of a case and review of the literature. Pediatr Dev Pathol 2008;11:239–244.
11 Somers GR, Shago M, Zielenska M, *et al.* Primary subcutaneous primitive neuroectodermal tumor with aggressive behavior and an unusual karyotype: case report. Pediatr Dev Pathol 2004;7:538–545.
12 Yoshimoto M, Graham C, Chilton-MacNeill S, *et al.* Detailed cytogenetic and array analysis of pediatric primitive sarcomas reveals a recurrent CIC-DUX4 fusion gene event. Cancer Genet Cytogenet 2009;195:1–11.
13 Choi EY, Thomas DG, McHugh JB, *et al.* Undifferentiated small round cell sarcoma with t(4;19)(q35;q13.1) CIC-DUX4 fusion: a novel highly aggressive soft tissue tumor with distinctive histopathology. Am J Surg Pathol 2013;37:1379–1386.
14 Antonescu C. Round cell sarcomas beyond Ewing: emerging entities. Histopathology 2014;64:26–37.
15 Specht K, Sung YS, Zhang L, *et al.* Distinct transcriptional signature and immunoprofile of CIC-DUX4 fusion-positive round cell tumors compared to EWSR1-rearranged ewing sarcomas: further evidence toward distinct pathologic entities. Genes Chromosomes Cancer 2014;53:622–633.
16 Wang L, Bhargava R, Zheng T, *et al.* Undifferentiated small round cell sarcomas with rare EWS gene fusions: identification of a novel EWS-SP3 fusion and of additional cases with the EWS-ETV1 and EWS-FEV fusions. J Mol Diagn 2007;9:498–509.
17 Sumegi J, Nishio J, Nelson M, *et al.* A novel t(4;22)(q31;q12) produces an EWSR1-SMARCA5 fusion in extraskeletal Ewing sarcoma/primitive neuroectodermal tumor. Mod Pathol 2011;24:333–342.
18 Szuhai K, Ijszenga M, de Jong D, *et al.* The NFATc2 gene is involved in a novel cloned translocation in a Ewing sarcoma variant that couples its function in immunology to oncology. Clin Cancer Res 2009;15:2259–2268.
19 Mastrangelo T, Modena P, Tornielli S, *et al.* A novel zinc finger gene is fused to EWS in small round cell tumor. Oncogene 2000;19:3799–3804.
20 Pierron G, Tirode F, Lucchesi C, *et al.* A new subtype of bone sarcoma defined by BCOR-CCNB3 gene fusion. Nat Genet 2012;44:461–466.
21 Puls F, Niblett A, Marland G, *et al.* BCOR-CCNB3 (Ewing-like) sarcoma: a clinicopathologic analysis of 10 cases, in comparison with conventional Ewing sarcoma. Am J Surg Pathol 2014;38:1307–1318.
22 Kim D, Salzberg SL. TopHat-Fusion: an algorithm for discovery of novel fusion transcripts. Genome biology 2011;12:R72.

23 McPherson A, Hormozdiari F, Zayed A, *et al.* deFuse: an algorithm for gene fusion discovery in tumor RNA-Seq data. PLoS Comput Biol 2011;7:e1001138.
24 Antonescu CR, Le Loarer F, Mosquera JM, *et al.* Novel YAP1-TFE3 fusion defines a distinct subset of epithelioid hemangioendothelioma. Genes Chromosomes Cancer 2013;52:775–784.
25 Lee CH, Ou WB, Marino-Enriquez A, *et al.* 14-3-3 fusion oncogenes in high-grade endometrial stromal sarcoma. Proc Natl Acad Sci USA 2012;109:929–934.
26 Robinson DR, Wu YM, Kalyana-Sundaram S, *et al.* Identification of recurrent NAB2-STAT6 gene fusions in solitary fibrous tumor by integrative sequencing. Nat Genet 2013;45:180–185.
27 Stein-Wexler R. Pediatric soft tissue sarcomas. Semin Ultrasound CT MR 2011;32:470–488.
28 Newton WA Jr., Soule EH, Hamoudi AB, *et al.* Histopathology of childhood sarcomas, intergroup rhabdomyosarcoma studies I and II: clinicopathologic correlation. J Clin Oncol 1988;6:67–75.
29 Rossiter JP, Young M, Kimberland ML, *et al.* Factor VIII gene inversions causing severe hemophilia A originate almost exclusively in male germ cells. Hum Mol Genet 1994;3:1035–1039.
30 Fan Z, Yamaza T, Lee JS, *et al.* BCOR regulates mesenchymal stem cell function by epigenetic mechanisms. Nat Cell Biol 2009;11:1002–1009.
31 Yamamoto Y, Tsuzuki S, Tsuzuki M, *et al.* BCOR as a novel fusion partner of retinoic acid receptor alpha in a t(X;17)(p11;q12) variant of acute promyelocytic leukemia. Blood 2010;116:4274–4283.
32 Panagopoulos I, Thorsen J, Gorunova L, *et al.* Fusion of the ZC3H7B and BCOR genes in endometrial stromal sarcomas carrying an X;22-translocation. Genes Chromosomes Cancer 2013;52:610–618.
33 Antonescu CR, Sung YS, Chen CL, *et al.* Novel ZC3H7B-BCOR, MEAF6-PHF1, and EPC1-PHF1 fusions in ossifying fibromyxoid tumors–molecular characterization shows genetic overlap with endometrial stromal sarcoma. Genes Chromosomes Cancer 2014;53:183–193.

Supplementary Information accompanies the paper on Modern Pathology website (http://www.nature.com/modpathol)